ACS OMEGA

Open Access

http://pubs.acs.org/journal/acsodf

Article

Inulin Inhibits the Inflammatory Response through Modulating Enteric Glial Cell Function in Type 2 Diabetic Mellitus Mice by Reshaping Intestinal Flora

Meng-Ying Li, Jia-Qi Duan, Xiao-Hui Wang, Meng Liu, Qiao-Yi Yang, Yan Li, Kun Cheng, Han-Qiang Liu,* and Feng Wang*

Cite This: *ACS Omega* 2023, 8, 36729−36743

Read Online

ACCESS | Metrics & More | Article Recommendations | Supporting Information

ABSTRACT: Inulin, a commonly used dietary fiber supplement, is capable of modulating the gut microbiome. Chronic inflammation resulting from metabolic abnormalities and gut flora dysfunction plays a significant role in the development of type 2 diabetes mellitus (T2DM). Our research has demonstrated that inulin administration effectively reduced colonic inflammation in T2DM mice by inducing changes in the gut microbiota and increasing the concentration of butyric acid, which in turn modulated the function of enteric glial cells (EGCs). Experiments conducted on T2DM mice revealed that inulin administration led to an increase in the *Bacteroidetes*/*Firmicutes* ratio and the concentration of butyric acid in the colon. The anti-inflammatory effects of altered gastrointestinal flora and its metabolites were further confirmed through fecal microbiota transplantation. Butyric acid was found to inhibit the activation of the κB inhibitor kinase β/nuclear factor κB pathway, regulate the expression levels of interleukin-6 and tumor necrosis factor-α, suppress the abnormal activation of EGCs, and prevent the release of inflammatory factors by EGCs. Similar results were observed in vitro experiments with butyric acid. Our findings demonstrate that inulin, by influencing the intestinal flora, modifies the activity of EGCs to effectively reduce colonic inflammation in T2DM mice.

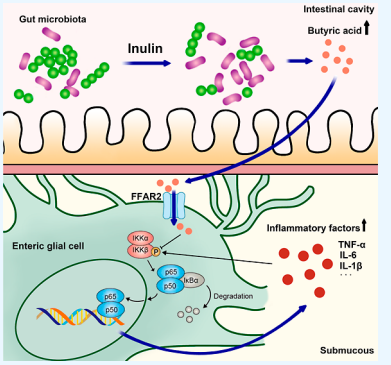

INTRODUCTION

The number of diabetes patients has been on the rise since 2019, and it is projected that by 2045, there will be a staggering 700 million individuals worldwide with diabetes, with type 2 diabetes mellitus (T2DM) accounting for the majority.[1] Numerous microorganisms inhabit the human skin, oral cavity, respiratory tract, and intestinal cannel and may modulate organ and system functions and maintain human health.[2] However, patients with diabetes exhibit evident dysregulation of the gut flora, characterized by an increase in Gram-negative bacteria capable of releasing lipopolysaccharide (LPS) and triggering inflammatory responses. Additionally, there is a decrease in protective and anti-inflammatory gut mucosal microbiota, further exacerbating the chronic systemic inflammatory response. Previous studies have demonstrated the significant involvement of chronic inflammation, induced by metabolic abnormalities and disturbances in the intestinal flora, in the pathogenesis of T2DM.[3,4]

Recent research on the enteric nervous system (ENS) has primarily focused on enteric neurons, leaving a scarcity of research on enteric glial cells (EGCs), particularly in the context of metabolic disorders. Pathological activation of EGCs can lead to similar alterations observed in the proliferation of reactive astrocytes in the central nervous system (CNS), which may play a pivotal role in the exacerbation of colonic and systemic inflammation.[5−7] However, the relationship between colonic inflammation, EGCs, and the development of T2DM has received limited attention, and many questions remain unanswered. Considering the interplay among intestinal flora, its metabolites, inflammation, and EGCs, as well as their regulatory effects on the human body environment, EGCs may emerge as a novel target for intervention and prevention of various diseases, including T2DM.

Inulin, a water-soluble dietary fiber, is classified as a polysaccharide and is found in approximately 36,000 plant species. Among them, chicory root is the most abundant source of inulin. Inulin serves as a substrate for the metabolism of various microorganisms and exerts its effects throughout the entire colon. It is commonly used as a prebiotic to develop functional foods that promote health. Previous studies have demonstrated the beneficial effects of dietary fiber on insulin resistance, regulation of glycolipid metabolism, modulation of intestinal flora, and reduction of inflammation.[8] Inulin undergoes degradation and fermentation by intestinal microorganisms, particularly in the colon, resulting in the production of

Received: May 3, 2023
Accepted: September 13, 2023
Published: September 28, 2023

short-chain fatty acids (SCFAs). Inulin exerts protective effects through multiple pathways, including reinforcement of the mucosal barrier, reduction of inflammatory factor release, and improvement of glucose homeostasis.[9,10] Inulin offers greater convenience, cost-effectiveness, and safety compared to pharmaceutical drugs, making it a valuable option for both the prevention and treatment of various intestinal flora abnormalities and inflammation-related diseases. While inflammation plays a significant role in the development of T2DM, the focus on colonic inflammation in treatment and prevention strategies for T2DM is still lacking. It remains uncertain whether dietary fiber can effectively alleviate colon inflammation in individuals with T2DM. Therefore, it is imperative to further investigate the impact and underlying mechanism of inulin on the inflammatory response in individuals with diabetes.

The potential of inulin to inhibit colon inflammation in individuals with T2DM can be inferred through its regulation of the intestinal microbiota and associated metabolites. EGCs may also play a regulatory role in the inflammatory state induced by metabolic disorders and imbalanced intestinal flora in T2DM patients. To investigate the protective effects of inulin on colon inflammation in T2DM, we established a T2DM mouse model. The model was created by subjecting C57BL/6 mice to a high-fat diet and intraperitoneal streptozotocin (STZ) injections. The effects of inulin on colon inflammation and gut microbiota in T2DM mice were examined. Additionally, we assessed the impact of inulin and its metabolite, SCFAs, on the activation of EGCs to validate the proposed mechanism. These findings provide valuable insights for future population studies, interdisciplinary collaborations, and the development of prevention and treatment strategies for T2DM.

MATERIALS AND METHODS

Reagents. Inulin (NG, HPLC ≥92%), a highly soluble inulin (HSI) produced by BENEO-Orafti S.A. (Belgium), was obtained for our study. This natural inulin is derived from chicory roots and contains a blend of fructooligosaccharides with varying chain lengths (degree of polymerization, DP, ranging from 2 to 60), with an average DP exceeding 10. Acetic acid, propionic acid, and butyric acid for gas chromatography−mass spectrometry (GC−MS) analysis were procured from Fisher Scientific International Inc. Antibodies specific to κB inhibitor kinase β (IKKβ), nuclear factor κB inhibitor α (IκBα), nuclear factor κB (NF-κB), interleukin-1β (IL-1β), interleukin-6 (IL-6), tumor necrosis factor (TNF-α), and glial fibrillary acidic protein (GFAP) were purchased from Biogot Technology Co., Ltd. (Nanjing, China). Anti-CD4 antibody, anti-CD8 antibody, and a diaminobenzidine (DAB) kit were acquired from Servicebio Technology Co., Ltd. (Wuhan, China). Enzyme-linked immunosorbent assay (ELISA) kits for measuring mouse TNF-α, LPS, and insulin were obtained from Biorbyt Biotechnology Co., Ltd. An ELISA reagent for mouse glycated serum protein (GSP) manufactured by Rayto Life and Analytical Sciences Co., Ltd. (Shenzhen, China) was also used. Beyotime Biotech, Inc. (Shanghai, China) provided radio immunoprecipitation assay (RIPA) lysis buffer and bicinchoninic acid (BCA) protein quantification reagent. The nuclear and cytoplasmic protein extraction reagents were acquired from EnoGene Biotechnology Co., Ltd. (Nanjing, China). The HiPure Total RNA Mini Kit was purchased from Magen Biotechnology Co., Ltd. (Guangzhou, China), and the MagPure Soil DNA LQ Kit was purchased from Magen. The PrimeScript RT reagent and the TB Green Premix Ex Taq II were supplied by Takara Biotechnology Co., Ltd. (Tokyo, Japan). GLPG0974 was provided by Shanghai's Topscience Co., Ltd., STZ was produced by Sigma-Aldrich Trading Co., Ltd. (St. Louis, USA), and citric acid-sodium citrate buffer (0.1 mol/L, pH 4.5) was supplied by Scientific Phygene Co., Ltd. (Fuzhou, China).

Animal Experiments. Male C57BL/6 mice (6 weeks old) were obtained from the Animal Experiment Center of Air Force Military Medical University in Xi'an, China. The mice had ad libitum access to food and water. The feeds were obtained from Sino Biotechnology Co., Ltd. in Siping, China (Tables S1 and S2). After 1 week of acclimatization to the diet, the mice were randomly divided into 3 groups: the control group (Con group), the diabetes mellitus group (DM group), and the diabetes mellitus with inulin group (DM-I group), each comprising 24 mice. The Con group received a standard chow diet, while the DM and DM-I groups were fed a high-fat diet (51% energy from fat) to induce diabetes mellitus. In the 12th week, the DM and DM-I groups received intraperitoneal injections of 1% STZ in ice-cold citric acid−sodium citrate buffer (0.1 mol/L, pH 4.5) at a dosage of 130 mg/kg body weight. The Con group received intraperitoneal injections of citric acid−sodium citrate buffer as a control. After 72 h, the random tail vein blood glucose levels of mice in both the DM group and the DM-I group reached 16.7 mmol/L, indicating successful induction of diabetes. The DM-I group mice were then fed high-fat diets supplemented with 15% inulin for 9 weeks, while the diets of the other groups remained unchanged. Throughout the 22 week experiment, the body weight of the mice was assessed weekly, and random tail vein glucose levels were measured weekly for 9 weeks after STZ administration. The experiment was approved by the Welfare and Ethics Committee of the Laboratory Animal Center of the Air Force Military Medical University under authorization number IACUC-20211051.

Test of Insulin Tolerance. During the 16th week of feeding, five mice were randomly selected from each group and subjected to a 4 h fasting period without access to water. Subsequently, an insulin solution was administered to each mouse. The insulin was injected intraperitoneally at a concentration of 0.2 IU/mL with a dose of 1 IU/kg. Following the injection, tail venous blood glucose levels were measured at 0, 15, 30, 60, 90, and 120 min.

Body Composition Examination. After 18 weeks, eight mice were randomly selected from each group and analyzed for lean and fat composition using a small animal component analyzer (Burker, Billerica, Germany).

Hematoxylin−Eosin (H&E) Staining and Immunohistochemical Analysis. Colon tissue samples were fixed in 4% paraformaldehyde, embedded in paraffin, and sectioned. Some sections were stained with hematoxylin and eosin (H&E), while the remaining sections were incubated with 5% bovine serum albumin (BSA) for 10 min at room temperature. Subsequently, the sections were incubated overnight with anti-CD4 antibody and anti-CD8 antibody (dilution: 1:200), respectively. The antibody binding sites were visualized using a DAB kit. All sections were examined under a light microscope (Olympus, Tokyo, Japan). The number of $CD4^+$ and $CD8^+$ cells was quantified using ImageJ software (NIH, Bethesda, USA).

Enzyme-Linked Immunosorbent Assay. The levels of LPS and TNF-α in mouse serum samples were determined using an ELISA reagent. Each well was filled with 100 μL of serum, and the absorbance at a wavelength of 450 nm was measured. Based

https://doi.org/10.1021/acsomega.3c03055
ACS Omega 2023, 8, 36729−36743

on these measured values, a standard curve was constructed, and the concentration of the target proteins was calculated.

Western Blot Evaluation. Total protein was extracted from mouse colon tissue by using RIPA lysis buffer. Nuclear and cytoplasmic proteins were isolated using specific extraction kits. Protein concentration was determined with a BCA protein quantification reagent. The protein sample was transferred from the sodium dodecyl-sulfate polyacrylamide gel electrophoresis gel to a PVDF membrane through electrotransfer after electrophoresis. The membrane was blocked with TBST (containing 5% skim milk) for 2 h at room temperature. Then, specific primary antibodies (IKKβ, *p*-IKKβ, IκBα, IL-1β, IL-6, NF-κB, and TNF-α, dilution: 1:1000) were incubated overnight at 4 °C. After rinsing with TBST, a secondary antibody was applied to the membrane for 2 h at room temperature. Protein bands were visualized and analyzed using a gel image analysis instrument (VILBER, Paris, France) and ImageJ software.

Real-Time Quantitative PCR Analysis. The HiPure Total RNA Mini Kit was employed for the extraction of the total RNA. Subsequently, cDNA was synthesized through reverse transcription. The prepared PCR solution and cDNA were then dispensed into PCR 8-strip tubes for RT-qPCR analysis. The primer sequences used in the experiment are provided in Table S3. The reaction conditions were as follows: stage 1: 95 °C for 30 s (once); stage 2: 95 °C for 5 s, 60 °C for 30 s (repeated for a total of 40 cycles).

16S rRNA Microbiome Sequencing. Fecal samples were collected at 9:00 am during the 21st week of feeding. Genomic DNA of the intestinal flora was extracted from the fecal samples using a DNA extraction kit. The bacterial 16S rRNA V3 V4 region was amplified using primers 343F (5′-TACGGRAGGCAGCAG-3′) and 798R (5′-AGGGTATCTAATCCT-3′). High-throughput sequencing of the 16S rRNA was conducted on an Illumina NovaSeq platform (OE Biotech, Shanghai, China). The primer sequence was removed using cutadapt software, resulting in double-ended sequence raw data. Quality filtering, noise reduction, splicing, and chimera removal were performed using DADA2 with the default parameters QIIME 2. This process generated representative sequences and their respective amplicon sequence variation abundances.

Fecal Bacteria Transplantation. 6 week old male C57BL/6 mice were divided into three groups: Con(FMT), DM(FMT), and DM-I(FMT), with 8 mice in each group. To deplete the gut microbiota, all mice were given drinking water containing an antibiotic cocktail (gentamicin 100 mg/L, ampicillin 1 g/L, erythromycin 10 mg/L, vancomycin 0.5 g/L, and neomycin 0.5 g/L) for 1 week. Fecal samples from the Con, DM, and DM-I groups were collected and suspended in sterile Ringer's solution (6% w/v). The suspension was filtered to remove large particles, and the filtrate was used for fecal bacteria transplantation. Each group of mice received an intragastric administration of the respective fecal bacterial suspension at a dose of 200 μL per day for 2 weeks. The preparation and transplantation procedures were completed within an hour.

SCFAs Analysis. The quantification of SCFAs, including acetic acid, propionic acid, and butyric acid, was conducted using ultra-performance liquid chromatography−electrospray ionization−tandem mass spectrometry (UPLC−ESI−MS/MS) analysis. Metabolite extraction methods were based on the chemical characteristics of the targeted metabolites. To extract the metabolites, 300 μL of a mixture of ice-cold acetonitrile and water (1:1, v/v), containing [2H9]-pentanoic acid and [2H11]-hexanoic acid as internal standards (IS), was added to 20 mg of freeze-dried feces. The mixture was then subjected to grinding with steel balls at a frequency of 60 Hz for 2 min. The resulting samples were further extracted by ultrasonication for 10 min in an ice−water bath and subsequently stored at −20 °C for 30 min. Afterward, the samples were centrifuged at 4 °C (13,000 rpm) for 10 min, and 80 μL of the supernatant was collected and transferred to sample vials. A Nexera UHPLC LC-30A system (SHIMADZU, Japan) was used for liquid chromatography analysis. An ACQUITY UPLC BEH C18 column (100 × 2.1 mm, 1.7 μm) with an injection volume of 5 μL was employed. The mobile phase consisted of water with 0.1% formic acid as solvent A and acetonitrile as solvent B. Mass spectrometry analysis was performed on an AB SCIEX Selex ION Triple Quad 5500 System (Ontario, Canada) using ESI in both positive and negative ion modes. Nitrogen was used as the collision gas.

The quantification of metabolites was carried out by using a triple quadrupole mass spectrometer in multiple reaction monitoring (MRM) mode. The formula used for calculating the metabolite concentration in the sample was as follows: sample metabolite concentration (ng/mL) = $5\,(C \times 0.16)/M$. In this formula, 5 is the dilution factor, C represents the concentration value obtained by fitting the peak area to a standard curve, 0.16 represents the injection volume, and M is the sample mass.

Whole Mount Stretch Preparation. The colon was perfused with a 4% paraformaldehyde solution to distension. Both ends of the colon were securely tied with surgical sutures and immersed in 4% paraformaldehyde for fixation under tension. After fixation, the colon was rinsed with phosphate-buffered saline (PBS) and then dehydrated in a 10% sucrose solution for 24 h. The intestinal lumen was delicately incised along the edge of the mesentery. Using an anatomical microscope, we sequentially peeled off the mucosal layer, submucosal layer, circular muscle layer, and longitudinal muscle layer.

Immunofluorescence Histochemical Staining. The submucosal layer of the colon was isolated and placed in a 24-well plate and mixed with a solution containing 3% BSA and 0.3% Triton X-100. The mixture was incubated at room temperature for 2 h. Primary antibodies (rabbit anti-NF-κB p65 antibody and mouse anti-GFAP antibody) diluted at a ratio of 1:200 were added to the plate and incubated overnight at 4 °C. A secondary antibody mixture consisting of Cy3-labeled goat antirabbit IgG (diluted at 1:500) and FITC-labeled goat antimouse IgG (diluted at 1:800) was then added and incubated in the dark at 37 °C for 1 h. The submucosa was transferred onto glass slides, dried in the dark at room temperature, and sealed with an antifluorescence quencher. Fluorescence signals were observed and captured by using a fluorescence microscope (Olympus, Tokyo, Japan), and ImageJ software was used for analysis.

Culture of Cells and Treatment. The EGCCRL-2690 EGC line was obtained from the ATCC cell bank in the US and cultured in DMEM supplemented with 10% FBS and 1% penicillin−streptomycin. The cells were maintained in a 37 °C humidified incubator with 5% CO_2. To induce insulin resistance and inflammation, EGCs were treated with 60 μg/mL LPS and 0.2 mM palmitic acid (PA) for 48 h. The cells were then treated with acetic and butyric acids at concentrations determined from animal experiments (acetic acid: Con dose group 39.5 μg/mL; DM dose group 9.8 μg/mL; and DM-I dose group 17.1 μg/mL; butyric acid: Con dose group 9.7 μg/mL; DM dose group 1.0

https://doi.org/10.1021/acsomega.3c03055
ACS Omega 2023, 8, 36729−36743

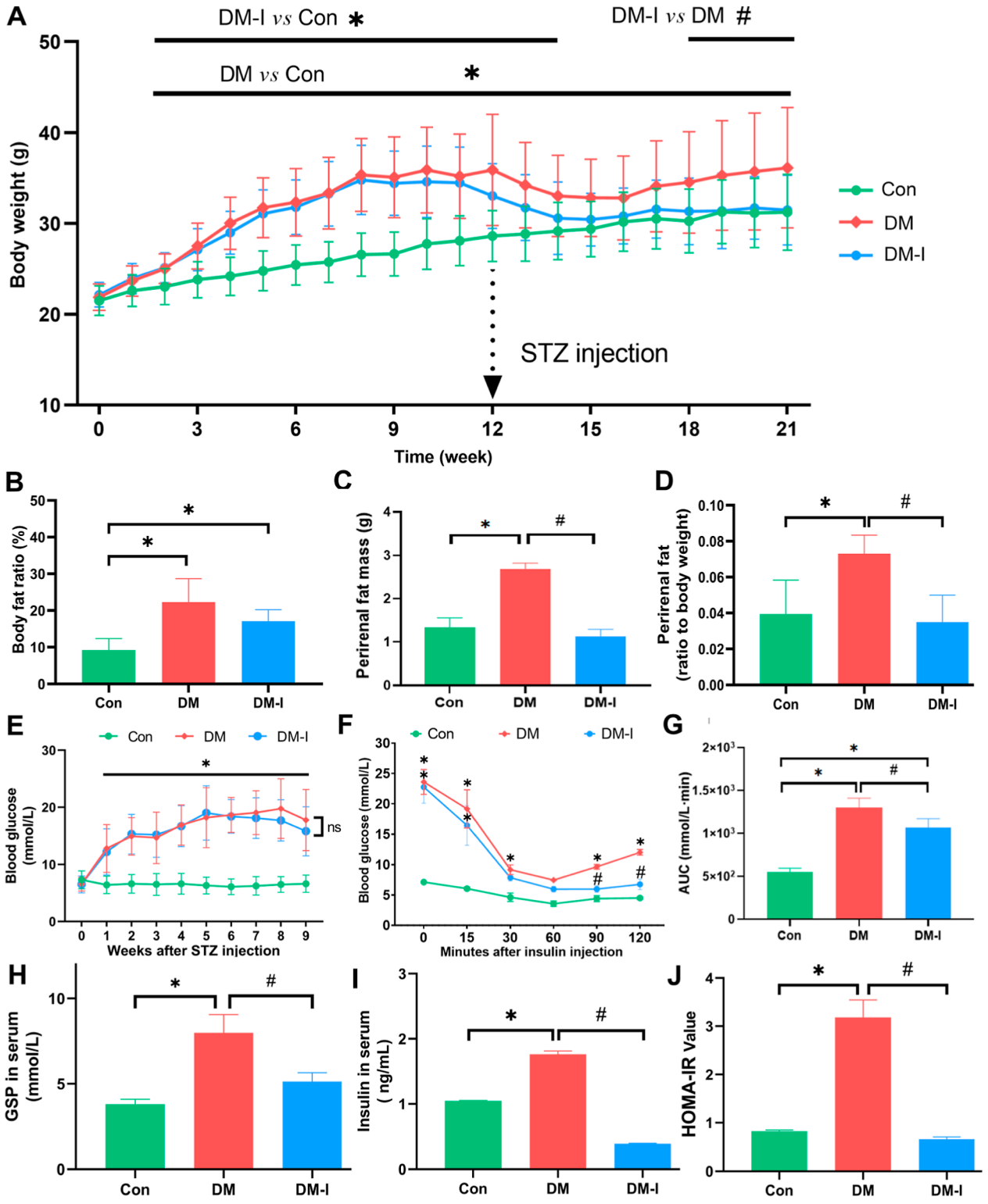

Figure 1. Inulin reduced body weight and abnormal glucose metabolism in T2DM mice. (A) Body weight of each group of mice ($n = 24$). (B) Ratio of body fat to body weight of mice at the 18th week. ($n = 8$). (C) Perirenal fat mass in each group of mice at the 22nd week ($n = 24$). (D) Perirenal fat mass to body weight ratio at the 22nd week ($n = 24$). (E) Blood glucose levels in each group of mice following an intraperitoneal injection of STZ ($n = 24$). (F,G) Insulin tolerance test was performed to evaluate the blood glucose levels and the corresponding area under the curve after insulin injection ($n = 5$). (H–J) GSP levels, fasting insulin levels, and HOMA-IR values were measured in each group ($n = 5$). The results are provided as means standard deviations, with $^{*}p < 0.05$ compared to the Con group and $^{\#}p < 0.05$ compared to the DM group.

μg/mL; DM-I dose group 2.3 μg/mL). EGCs maintained in a normal medium served as the control group. To confirm the anti-inflammatory effect of butyric acid in EGCs, GLPG0974, a selective antagonist of free fatty acid receptor 2 (FFAR2), was added to the culture medium at a concentration of 90 nM. The EGCs were cultured in complete medium for 24 h, followed by 48 h of culture in medium containing 0.2 mM PA, 60 μg/mL LPS, 2.3 μg/mL butyric acid, and 90 nM GLPG0974.

https://doi.org/10.1021/acsomega.3c03055
ACS Omega 2023, 8, 36729−36743

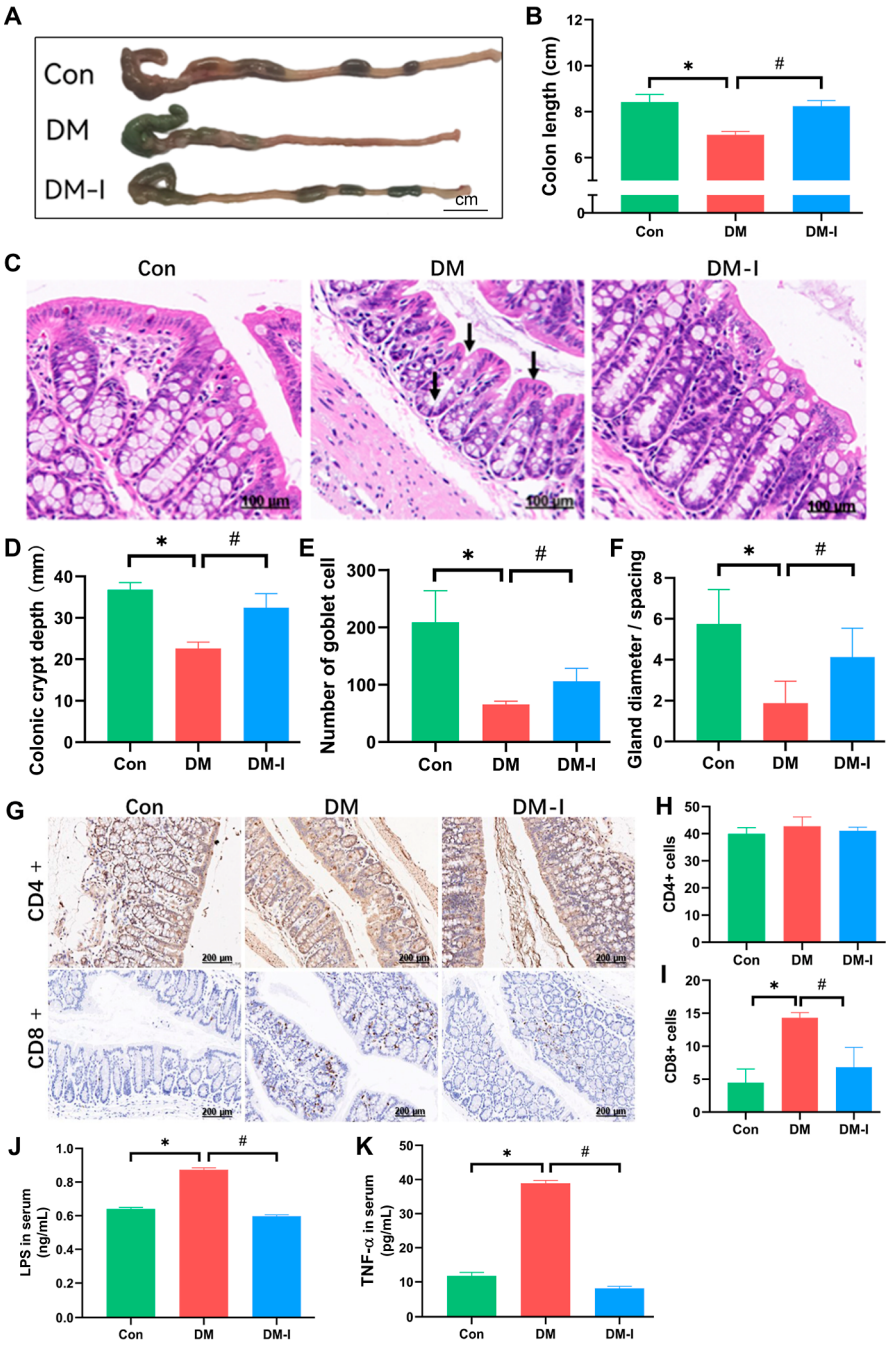

Figure 2. Inulin intake reduced colon and systemic inflammation in T2DM mice. (A,B) Colon length of each group of mice ($n = 24$). (C−F) At the 22nd week, the representative H&E staining of colon sections, the depth of colonic crypts, the number of goblet cells, and the ratio of transverse diameter to gland spacing in each group of mice ($n = 3$). (G−I) Number of $CD4^+$ and $CD8^+$ cells in the colon at the end of the intervention ($n = 3$). (J,K) LPS and TNF-α levels in mouse serum ($n = 3$). The results are provided as means standard deviations, with $^*p < 0.05$ compared to the Con group and $^{\#}p < 0.05$ compared to the DM group.

Cell-Attached Slide. EGCs were seeded at a density of 5×10^4 cells/mL on a sterile glass slide placed in a 12-well plate and cultured at 37 °C with 5% CO_2 for 24 h to allow attachment. Each well was assigned to one of four groups: control, LPS + PA (0.2 mM PA and 60 μg/mL LPS), acetic acid (0.2 mM PA, 60 μg/mL LPS, and 17.1 μg/mL acetic acid), and butyric acid (0.2 mM PA, 60 μg/mL LPS, and 2.3 μg/mL butyric acid). The corresponding medium was added to each well, and the cells were cultured for an additional 48 h. Afterward, the specimens were removed for immunofluorescence staining using the same method as described for the colonic submucosa.

Methods for Statistical Processing. All data are represented by the formula mean ± standard deviation (M ± SD). GraphPad Prism 8 was used for the statistical analysis. A nonparametric test was used to compare statistical differences between groups. A one-way ANOVA with Tukey's multiple comparison test was used to evaluate statistical differences between multiple groups. The level of statistical significance was set at $p < 0.05$.

https://doi.org/10.1021/acsomega.3c03055
ACS Omega 2023, 8, 36729−36743

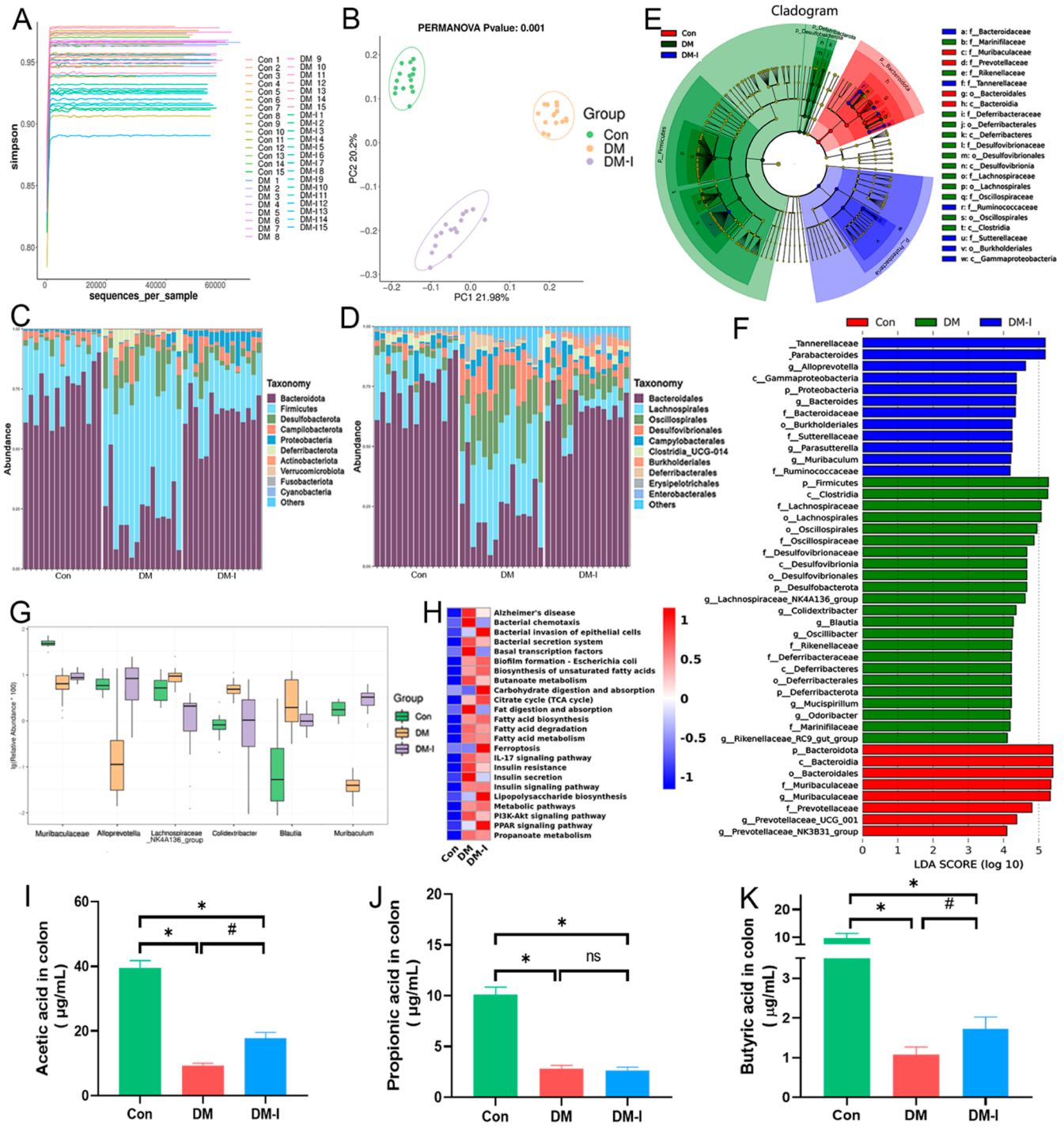

Figure 3. Inulin reversed the intestinal flora imbalance and up-regulated the levels of acetic acid and butyric acid in the colon of T2DM mice. (A) Simpson's index for alpha diversity (n = 15). (B) Beta diversity of gut microbiota among different groups was revealed through PCoA based on amplified sequence variant data. (n = 15). (C) Composition and abundance of gut bacteria at the phylum level for each group (n = 15). (D) Intestinal bacterial composition and abundance at the order level (n = 15). (E) LEfSe analysis for each group of mice (n = 15). (F) Key intestinal bacteria phylotypes from each group (n = 15). (G) Genus-level composition of gut bacteria (n = 15). (H) Heatmap of KEGG differential result clustering (n = 15). (I–K) Acetic acid, propionic acid, and butyric acid content in the colon of mice in each group (n = 15). Results are presented as mean ± SD, $^{*}p < 0.05$ compared to the Con group, $^{\#}p < 0.05$ compared to the DM group.

RESULTS

Inulin Reduced Body Mass and Visceral Fat in Mice with T2DM. As depicted in Figure 1A, mice in the DM and DM-I groups displayed significantly higher body weight compared to mice in the Con group after 3 weeks on a high-fat diet. Following STZ injection, the DM-I mice were fed a high-fat diet supplemented with inulin. At the 18th week, a notable disparity in body weight was observed between DM-I mice and DM mice, despite the fact that their energy intake was identical (Figure S1A,B). To investigate the underlying cause of this weight difference, we analyzed the body composition of the mice. Although the average body fat percentage of DM-I mice was

https://doi.org/10.1021/acsomega.3c03055
ACS Omega 2023, 8, 36729−36743

lower than that of DM mice, the difference was not statistically significant (Figure 1B). However, after 22 weeks of nutrition, a significant difference in perirenal fat mass and ratio between DM mice and DM-I mice was observed (Figure 1C,D). These findings are consistent with previous studies[12,13] and suggest that inulin supplementation reduces body weight and visceral fat in mice with high-fat diet-induced T2DM following STZ administration.

Inulin supplementation improved insulin sensitivity in mice with T2DM. As depicted in Figure 1E, the blood glucose levels of mice in the DM and DM-I groups significantly increased following STZ injection compared with the control group. However, there was no significant difference in blood glucose levels between DM-I and DM mice until 9 weeks after STZ injection and inulin consumption. The insulin tolerance test revealed that DM-I mice exhibited a more substantial decrease in blood glucose levels compared to DM mice after receiving the same dose of insulin, and the area under the curve was significantly different (Figure 1F,G). Measurement of GSP, fasting insulin levels, and HOMA-IR values further demonstrated enhanced glucose metabolism in the DM-I group compared with the DM group (Figure 1H−J). These findings are consistent with previous studies,[14] indicating that inulin supplementation can increase insulin sensitivity in mice with T2DM induced by a high-fat diet and STZ administration.

Mice with T2DM that were administered inulin exhibited reduced colonic and systemic inflammation. Colonic inflammation is characterized by significant manifestations such as colon shortening, colonic sac disappearance, and shallowness. The length of the colon in DM mice was considerably shorter compared to that of Con mice, but this difference was statistically significant and was restored in the DM-I group (Figure 2A,B). Histological examination revealed significant pathological changes in the colon of diabetic mice. These changes included a decrease in goblet cells and intracellular crypt mucus, atrophy and distortion of crypts with varying lumen sizes, enlarged crypt openings, irregular mucosal surfaces, and finger-like alterations. The inclusion of inulin in the diet mitigated the severity of these inflammatory pathological alterations (Figure 2C−F). Furthermore, the results of periodic acid-Schiff (PAS) staining and counting of colonic goblet cells exhibited a consistent trend (Figure S2A,B). Similarly, immunohistochemical staining indicated a lower number of $CD8^+$ cells in the colon of DM-I mice compared to DM mice, while there was no significant difference in the number of $CD4^+$ cells among the three groups (Figure 3G−I). Furthermore, the levels of inflammatory factors in the serum were measured. ELISA analysis revealed that serum LPS and TNF-α levels were significantly higher in DM mice compared to Con mice, but no significant differences were observed between DM-I and Con mice (Figure 2J,K). Based on our findings, we concluded that inulin alleviates colon and systemic inflammation in mice with T2DM.

Inulin Corrected the Intestinal Bacterial Imbalance in T2DM Mice. Each mouse group's feces were collected for 16S rRNA sequencing. As shown in Figure 3A, the Simpson index, used to assess alpha diversity, was lower in the DM-I group of mice, indicating changes in the composition and structure of the gut microbial community in the DM-I group. This suggests a potential reduction or loss of certain microbial species, thereby decreasing the diversity of the community. However, despite the reduced microbial diversity, functional remodeling of the microbial community resulted in an improved health status for the organisms. Principal coordinate analysis (PCoA) showed distinct clustering of the intestinal flora among the Con, DM, and DM-I groups (Figure 3B). These results indicate significant differences in the beta diversity and composition of the intestinal microbial community among the different groups of mice. As shown in Figure 3C,D, additional analysis suggested that dietary inulin can reverse the alterations of intestinal flora in the DM group, specifically by increasing *Bacteroidetes* and decreasing *Firmicutes*. At the genus level, inulin ingestion significantly increased the abundance of *Muribaculaceae*, *Alloprevotella*, and *Muribaculum* while decreasing the abundance of the *Lachnospiraceae*_NK4A136_group, *Colidextribacter*, and *Blautia* (Figure 3G). Linear discriminant analysis effect size (LEfSe) analysis revealed that inulin administration effectively regulated the relative abundance of diverse intestinal microbes, as shown in Figure 3E,F. Additionally, the Kyoto Encyclopedia of Genes and Genomes (KEGG) function prediction, based on 16S rRNA sequencing, demonstrated significant correlations between changes in the intestinal flora of T2DM mice and various factors, including nervous system diseases, bacterial biological function, butyric acid metabolism, and insulin resistance, as depicted in Figure 3H. These findings collectively suggest that inulin has the potential to modulate the composition of the intestinal flora and ameliorate the imbalance in mice with T2DM.

Inulin Increased the Amount of Acetic Acid and Butyric Acid in the Colon of Mice with T2DM. SCFAs are crucial byproducts generated through the microbial fermentation of dietary fiber in the colon. Consistent with the KEGG analysis findings, which indicated a connection between the alteration in the intestinal flora of T2DM mice after inulin administration and butyric acid metabolism, we investigated the levels of major inulin metabolites, including acetic, propionic, and butyric acids, in the colon of each experimental group. The results revealed a significant decrease in the SCFA concentration in the colons of diabetic mice. Although there was a partial recovery in the levels of acetic and butyric acids following inulin consumption, they remained significantly different from those observed in the Con group. Notably, the levels of propionic acid did not show significant changes (Figure 3I−K). Based on these findings, we conclude that inulin consumption has the potential to enhance SCFA concentration in the colon of T2DM mice, particularly acetic acid and butyric acid.

Inulin Inhibits the NF-κB Inflammatory Pathway in T2DM Mice's Colon. NF-κB is a transcription factor that plays a crucial role in various biological processes, including inflammation, immune response, apoptosis regulation, and stress response. Excessive activation of the NF-κB signaling pathway is associated with the development and progression of inflammation. Previous studies have shown that SCFAs can inhibit activation of the NF-κB signaling pathway, leading to a decrease in the release of inflammatory factors and an increase in the production of anti-inflammatory factors. Through Western blot analysis, we observed the activation of the IKKβ/NF-κB pathway in colon tissues. The ratio of pIKKβ/IKKβ was higher in the DM and DM-I groups compared to the Con group, resulting in the degradation of IκBα and a significant increase in the nuclear translocation of NF-κB. However, in the DM-I group, compared to the DM group, phosphorylation of IKKβ was inhibited, leading to a reduction in the nuclear translocation of NF-κB. Additionally, dietary supplementation with inulin significantly decreased the levels of IL-1β, IL-6, and TNF-α in DM mice, as shown in Figure 4A−C. Real-time quantitative

https://doi.org/10.1021/acsomega.3c03055
ACS Omega 2023, 8, 36729−36743

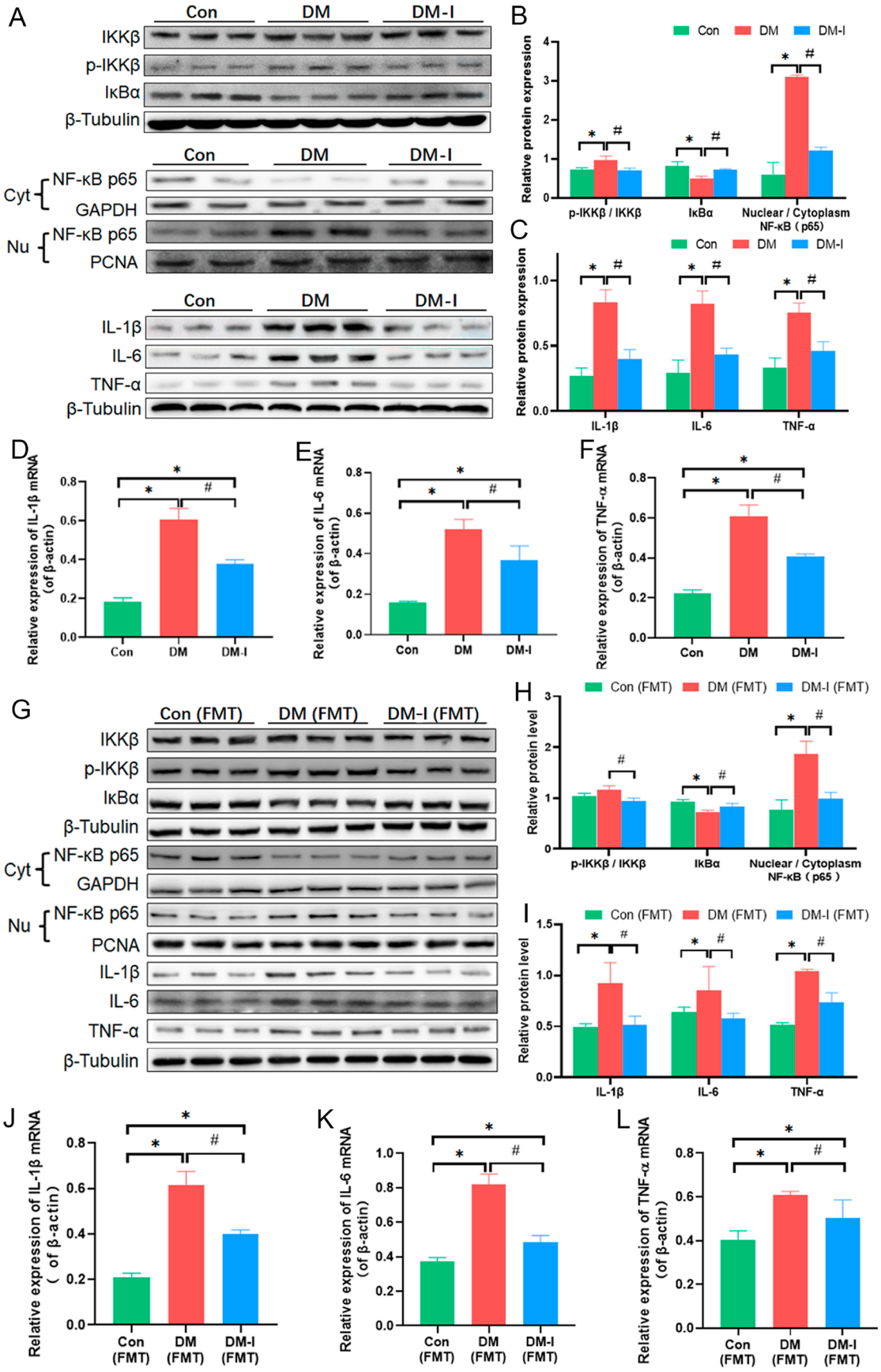

Figure 4. Inulin reduced inflammatory response in T2DM mice by inhibiting NF-κB nuclear translocation. (A−C) IKK*β*, *p*-IKK*β*, IκB*α*, NF-κB (in the nucleus and cytoplasm), IL-1*β*, IL-6, and TNF-*α* expression in the colon of Con, DM, and DM-I mice (n = 3). (D−F) Inflammatory factor gene expression (IL-1*β*, IL-6, and TNF-*α*) (n = 3). (G−I) Protein expression in mice after FMT from the Con, DM, and DM-I groups (n = 3). (J−L)

https://doi.org/10.1021/acsomega.3c03055
ACS Omega 2023, 8, 36729−36743

Figure 4. continued

Inflammatory factor gene expression (IL-1β, IL-6, and TNF-α) in mice after FMT ($n = 3$). Results are presented as mean ± SD, $^{*}p < 0.05$ compared to the Con group, $^{\#}p < 0.05$ compared to the DM group.

PCR analysis showed a significant increase in mRNA levels of IL-1β, IL-6, and TNF-α in the colon of mice in the DM group. However, the addition of inulin to the diet led to a decrease in the mRNA transcription levels of these inflammatory factors. Importantly, the difference in mRNA levels between the inulin-treated group and the Con group remained significant (Figure 4D−F). Based on these findings, we concluded that the protective effect of inulin on colon inflammation in T2DM mice is achieved through the regulation of intestinal flora and subsequent changes in SCFA content. To further validate this hypothesis, we performed fecal microbiota transplantation (FMT). Figure 4G−I demonstrates the activation of the NF-κB pathway and elevated levels of inflammatory factors in DM(FMT) mice that received FMT from the DM group. In contrast, DM-I(FMT) mice that received FMT from the DM-I group showed a decrease in nuclear translocation of NF-κB and levels of inflammatory factors compared to DM(FMT) mice. The expression of inflammatory factor mRNAs reflected these changes (Figure 4J−L). These findings provide strong evidence that inulin supplementation effectively inhibits NF-κB inflammatory pathways and reduces the levels of inflammatory factors in the colon of T2DM mice.

Butyric Acid Regulated EGC Function to Decrease Colonic Inflammation. EGCs play a vital role in maintaining intestinal function and have been shown to regulate the inflammatory process. Numerous studies have demonstrated that the NF-κB pathway serves as a fundamental mechanism by which these cells modulate inflammation.[15] To investigate the mechanism behind the mitigation of colonic inflammation in T2DM mice, we proposed a hypothesis that inulin inhibits the activation of the NF-κB pathway by modulating the function of EGCs via SCFAs. To test this hypothesis, we exposed mice to a high-fat diet for a short period. After 4 weeks of the high-fat diet, we observed the activation of EGCs, marked by increased expression of the GFAP. However, the protein levels of IL-6 and TNF-α at the corresponding time points did not show significant differences compared to the Con group (Figure 5A,B). This led us to propose that abnormal activation of EGCs may be the cause of colonic inflammation in mice. To further investigate this, we used immunofluorescence histochemistry with a whole-mount stretch preparation to stain EGCs in the submucosa of the colon. Compared to the DM-I group, the translocation of NF-κB p65 into the nucleus of EGCs in the colonic submucosal plexus was more pronounced in the DM group, indicating the activation of the NF-κB pathway in EGCs of T2DM mice (Figure 5C,D). In vitro experiments, varying concentrations of SCFAs extracted from the feces of each animal group were used. Butyric acid effectively inhibited the activation of the NF-κB pathway and increased the expression of inflammatory factors induced by LPS (Figure 5E−G). These effects were most prominent in the Con dose group, followed by the DM-I dose group, and finally the DM dose group. Acetic acid did not show any evidence of inflammation inhibition (Figure 5H−J). The immunofluorescence staining used to observe the nuclear translocation of NF-κB p65 within EGCs also demonstrated consistent results (Figure 6A,B). The anti-inflammatory effects of butyric acid were abolished when GLPG0974, a FFAR2 inhibitor, was added to the medium (Figure 6C−E). These findings suggest that inulin regulates the abnormal activation of EGCs by modulating the production of butyric acid by the intestinal flora, ultimately reducing the level of production of inflammatory factors through the inhibition of the NF-κB pathway.

DISCUSSION

Dietary Inulin Improved the Metabolism of Mice with T2DM Induced by a High-Fat Diet and STZ and Decreased Colonic Inflammation. In patients with T2DM, the intake of soluble dietary fiber has been shown to improve adiposity and insulin resistance. Inulin, a commonly used prebiotic, has also been reported to have beneficial effects on human health. In our study, we observed that dietary inulin supplementation improved glucose and lipid metabolism in T2DM mice, which is typically characterized by obesity, insulin resistance, and subsequent insulin secretion dysfunction. Furthermore, inulin administration led to a reduction in colonic and systemic inflammation. The most striking effects were observed in T2DM mice treated with inulin, as evidenced by weight loss, a decrease in the ratio of perirenal white fat to body weight, improved insulin sensitivity, amelioration of inflammatory changes in the crypts, goblet cells, and mucosal surface of the colon observed through H&E staining, as well as a decrease in the levels of inflammatory markers such as LPS and tumor necrosis TNF-α in the peripheral circulation. Interestingly, even in the presence of abnormal blood glucose levels, inulin consumption resulted in reduced body weight and visceral fat ratio in mice fed a high-fat diet, which partially explains the observed enhancement in insulin sensitivity in the inulin-fed experimental animals.

Currently, the role of the inflammatory response in promoting the pathological processes in T2DM and its impact on affected tissues and organs is well recognized. Several studies have provided insights into the mechanisms by which T2DM induces inflammation and oxidative stress.[16−20] It is indisputably beneficial to modulate the inflammatory response in T2DM patients.[21−25] The cardiovascular, renal, and other organ-protective effects of novel antidiabetic medications have been attributed to their anti-inflammatory properties.[26] Colonic inflammation, with its detrimental effects on the mucosal barrier, bacterial infection, and insulin resistance, has been implicated in various diseases, including diabetes. A growing body of evidence has shown an association between the development of T2DM and its complications with a state of chronic inflammation.[27,28] Intestinal inflammation leads to increased intestinal permeability, triggering a cascade of events, such as infection and systemic inflammation.

We selected inulin as the water-soluble dietary fiber source for our study based on its multifunctional properties and established market availability. The literature suggests that 37 g/kcal[11] of inulin was added to the experimental diet. However, it is yet to be determined whether this dosage is optimal for the prevention and treatment of colonic inflammation in T2DM mice.

In mice with T2DM, inulin remodeled the intestinal flora imbalance and increased the levels of acetic and butyric acid.

https://doi.org/10.1021/acsomega.3c03055
ACS Omega 2023, 8, 36729−36743

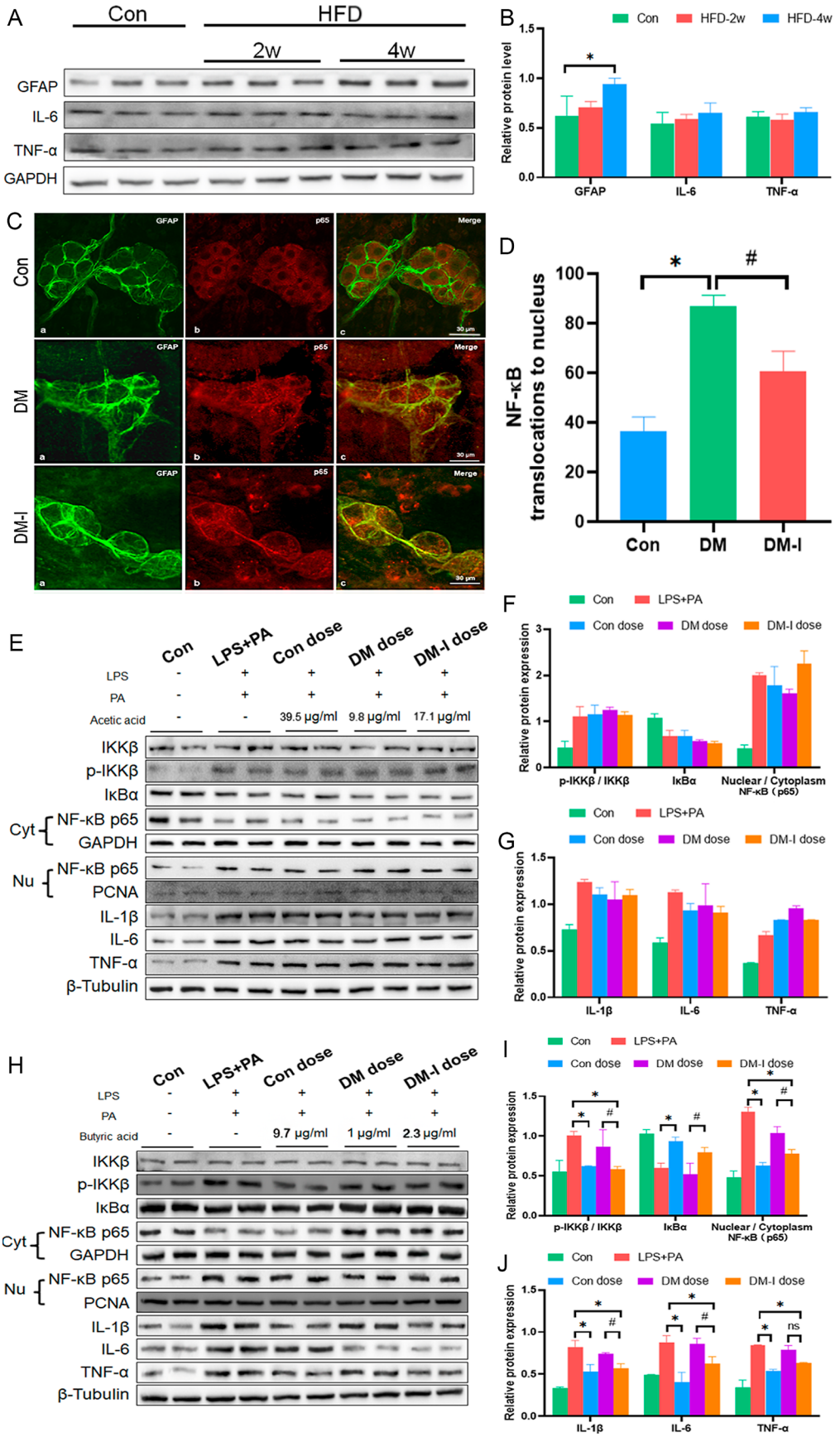

Figure 5. Butyric acid regulates the function of EGCs to reduce colonic inflammation. (A,B) GFAP, IL-6, and TNF-α protein levels in the colon of mice fed a high-fat diet for 2 or 4 weeks (n = 3). (C,D) Immunofluorescence analysis of NF-κB p65 translocation to the nucleus in EGCs in the colonic submucosa of mice (n = 3). (E−G) Inhibitory effect of different dosages of acetic acid (from animal trials) on LPS-induced inflammatory response in

https://doi.org/10.1021/acsomega.3c03055
ACS Omega 2023, 8, 36729−36743

Figure 5. continued

the situation of insulin resistance produced by PA in cultured EGCs in vitro ($n = 3$). (H–J) Inhibitory effect of different doses of butyric acid (from animal experiments) on LPS-induced inflammatory response while PA induced insulin resistance ($n = 3$). Results are presented as mean ± SD, (B) *$p < 0.05$ compared to the Con group. (D) *$p < 0.05$ compared to the DM group. (F,G,I,J) *$p < 0.05$ compared to the LPS + PA group, $^{\#}p < 0.05$ compared to the DM dose group.

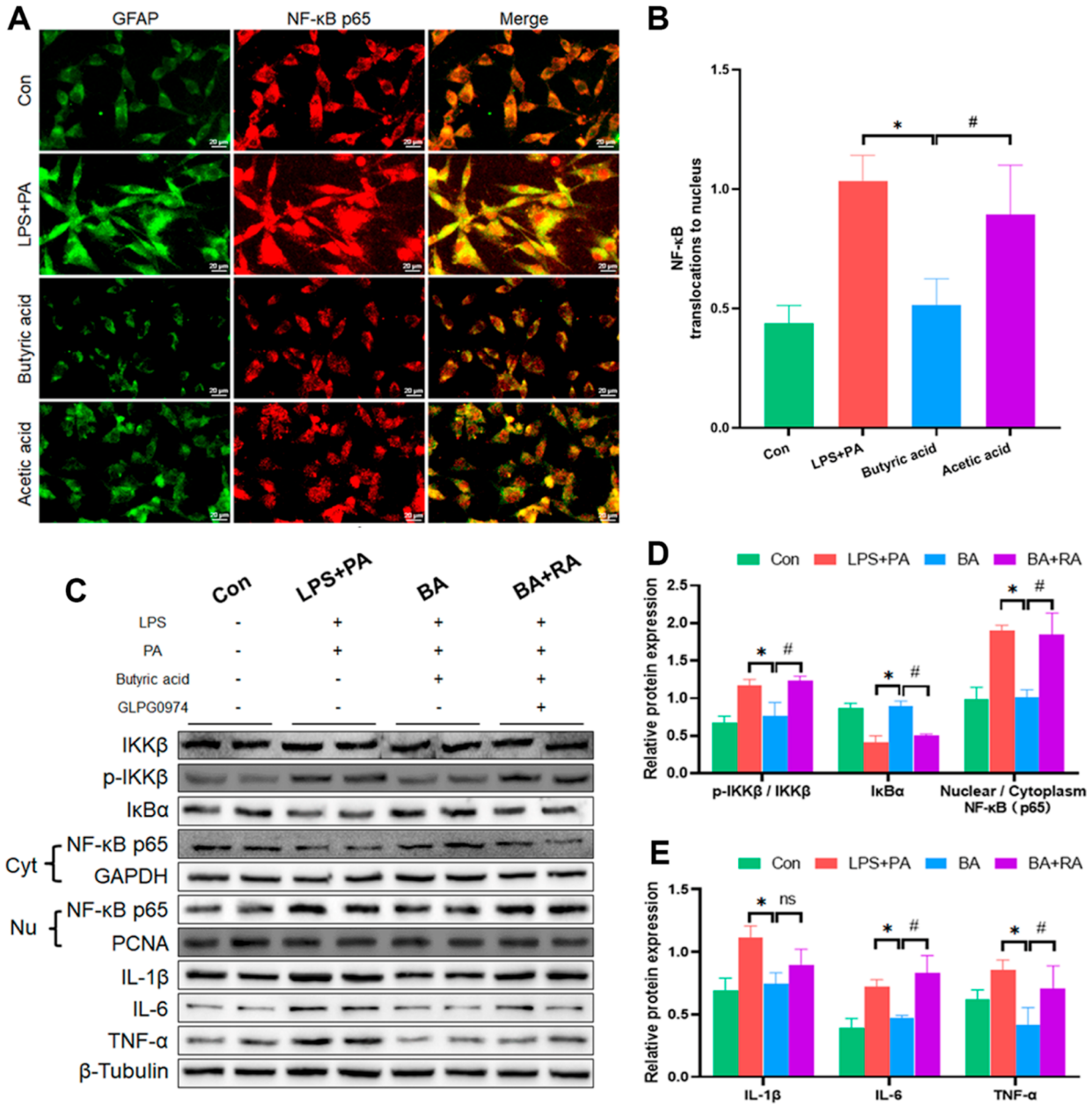

Figure 6. Butyric acid and GLPG0974 inhibited the activation of the NF-κB pathway in cultured EGCs in vitro. (A,B) Immunofluorescence was used to observe NF-κB p65 nucleus translocation in EGCs cultured in vitro with LPS and PA following intervention with acetic acid or butyric acid ($n = 3$). (C–E) Protein levels of NF-κB pathway-related factors and downstream inflammatory factors were measured by Western blotting in EGCs cultured in vitro with LPS and PA, treated with butyric acid (BA group) or both butyric acid and the free fatty acid receptor inhibitor GLPG0974 (BA + RA group) ($n = 4$). Results are presented as mean ± SD, (B) *$p < 0.05$ compared to the LPS + PA group, $^{\#}p < 0.05$ compared to the butyric acid group. (C–E) *$p < 0.05$ compared to the LPS + PA group, $^{\#}p < 0.05$ compared to the BA group.

In T2DM mice, dietary inulin reversed the disorder of intestinal flora and the reduction of SCFAs. It reversed the abnormally elevated *Bacteroidetes*/*Firmicutes* (B/F) ratio, narrowed the disparity between the abundance of other microorganisms, such as *Muribaculaceae*, and the Con group, and to some extent increased the concentrations of acetic and butyric acid. These modifications were presumably responsible for the decrease in colon and systemic inflammation in T2DM mice.

The intestinal microbiota plays a crucial role in the development of the immune system, defense against pathogenic microorganisms, digestion of exogenous substances, and

https://doi.org/10.1021/acsomega.3c03055
ACS Omega 2023, 8, 36729–36743

regulation of metabolism. In recent years, evidence has emerged regarding the distinctive characteristics of the intestinal microbiome in patients with metabolic diseases.[29] The dysbiosis of intestinal flora in patients with T2DM is primarily characterized by an abnormal ratio of *Bacteroidetes* to *Firmicutes*, with a notable enrichment in carbohydrate membrane transport and butyric acid biosynthesis functions.[30] Furthermore, the genetic information on these microorganisms is implicated in the oxidative stress process, indicating a direct association between alterations in the composition of the intestinal flora and the inflammatory state observed in T2DM patients.[31] The *Bacteroidetes*/*Firmicutes* (B/F) ratio in the colon of T2DM mice exhibited an increase, consistent with the trend observed in patients with various metabolic and inflammatory diseases, including obesity and nonalcoholic fatty liver disease. However, the addition of inulin to the diet of T2DM mice led to a significant decrease in the B/F ratio. Furthermore, the increased presence of *Colidextribacter*, a Gram-negative bacterium, was observed in the intestines of the DM group. This bacterium is considered a conditional pathogen and has the potential to induce inflammation. This likelihood was notably elevated in T2DM mice with a compromised intestinal mucosal barrier integrity. Moreover, an association has been established between the increased abundance of *Rikenellaceae* and stress, as well as inflammatory responses.[32] On the other hand, *Muribaculaceae* is generally recognized as a beneficial bacterium that exerts positive effects on intestinal energy metabolism and regulates the host's blood glucose and lipid levels.[33] However, in the DM group, there was a decrease in the abundance of *Muribaculaceae*. Additionally, the relative abundance of SCFA-producing bacteria, such as *Alloprevotella* and *Clostridia*, was lower compared to that of the Con group. The observed improvements in these phenomena in the DM-I group indicate that inulin intervention regulated the composition of intestinal flora in T2DM mice, alleviating the dysbiosis and offering protection for T2DM mice. Numerous studies have consistently shown that the influence of the intestinal microbiota on the host is a result of highly intricate processes, where the metabolites produced by microorganisms also impact the composition and functioning of the entire microbial community. Rather than focusing solely on alterations in the abundance of individual microorganisms, it is often more meaningful to consider the proportions and relationships among various members of the overall flora.

Dietary fibers, such as inulin, are indigestible and cannot be assimilated by the human body. However, it serves as a metabolic substrate for intestinal microorganisms during fermentation, leading to the production of SCFAs such as acetic, propionic, and butyric acid. The specific types and quantities of SCFAs generated are dependent on the intake of dietary fiber and the composition of the intestinal microbiota. Butyric acid, a metabolite of intestinal flora, plays a crucial role as an energy source for the colonic mucosa, facilitates nutrient synthesis, exhibits anti-inflammatory properties, and improves insulin activity, as indicated by numerous studies. The liver primarily absorbs acetic and propionic acids, which have significant effects on adipogenesis and gluconeogenesis. Emerging research suggests that SCFAs, important metabolites of dietary fiber, play various protective roles. For example, they help maintain intestinal barrier function and reduce the growth of pathogenic bacteria by decreasing intestinal pH.[34] SCFAs also activate peroxisome proliferators-activated receptor (PPAR) and mitogen-activated protein kinase (MAPK) signaling pathways, inhibit lipoprotein lipase,[35] enhance insulin sensitivity and glucose tolerance by sensing glucose through the gut−brain axis,[10] regulate appetite and energy balance by activating corresponding receptors, and exert anti-inflammatory effects both locally in the intestine and systemically. SCFAs serve as a crucial energy source for intestinal epithelial cells, thereby enhancing the integrity of the mucosal barrier. This, in turn, can lead to a reduced intestinal permeability and a subsequent decrease in systemic inflammation. Among the SCFAs, butyric acid emerges as the preferred energy source for colonic cells and exerts a significant impact on preserving the balance and functionality of the intestinal epithelium.[36]

Inulin Improved Colonic Inflammation in T2DM Mice by Inhibiting the IKKβ/NF-κB Pathway Activation. Inulin exhibits an anti-inflammatory effect by inhibiting the activation of the IKKβ/NF-κB pathway, leading to a reduction in the expression of IL-1β, IL-6, and TNF-α. Furthermore, the findings from FMT experiments indicate that inulin's inhibitory effect on the IKKβ/NF-κB pathway is achieved through the regulation and restoration of the composition of the intestinal microbiota.

NF-κB is an intracellular nuclear transcription factor that plays a critical role in regulating apoptosis, stress, and inflammatory and immune responses in the body. The activation of the NF-κB signaling pathway is closely linked to the inflammatory response, which can be excessive under certain conditions. The IKK signaling pathway is a prominent factor contributing to insulin resistance in peripheral tissues. IKKβ can enhance the activation of NF-κB, leading to the expression of TNF-α and IL-1β. Apart from their role in inducing inflammation, these cytokines also contribute to peripheral tissue insulin resistance.[37] Upon NF-κB activation, TNF-α and IL-1β utilize their respective receptors[38] to stimulate the NF-κB pathway, setting up a feedforward mechanism. Free fatty acids and a high glucose environment can activate NF-κB by triggering the production of TNF-α, IL-1β, and IL-6.[39] Inhibiting NF-κB activation has a protective effect on islet cells, safeguarding them from various detrimental effects.[40] The potential mechanisms by which the microbiota influences the metabolism of patients with T2DM include the regulation of the inflammatory response, modulation of intestinal permeability, influence on insulin sensitivity in key glucose metabolic organs such as the liver, skeletal muscle, and adipose tissue, and improvement of obesity by affecting fatty acid oxidation synthesis. The cross-talk between the intestinal microbiota and the host regulates local or systemic immunity and inflammation, which, in turn, contributes to the development of T2DM. Dysfunction of the intestinal barrier plays a crucial role in this process. The intestinal barrier serves to protect the body from the contents of the intestine, and its dysfunction leads to increased leakage of bacteria or their products, resulting in chronic inflammation and metabolic disorders.[41,42] Therefore, activation of the NF-κB pathway is crucial in the context of intestinal dysbiosis, obesity, and T2DM.

By Modulating the Function of EGCs, Inulin and Its Metabolite Butyric Acid Inhibited Colonic Inflammation. We initially established that the development of colonic inflammation in mice was attributed to the abnormal activation of EGCs. Subsequently, we observed that increased levels of butyric acid, a metabolite of inulin, hindered the nuclear translocation of NF-κB in insulin-resistant EGCs, leading to anti-inflammatory effects. Furthermore, the specific antagonist GLPG0974 for FFAR2 effectively blocked the regulatory effects of butyric acid on the NF-κB pathway in EGCs, thereby eliminating its anti-inflammatory capabilities. This finding further corroborates the significant role of altered biological

https://doi.org/10.1021/acsomega.3c03055
ACS Omega 2023, 8, 36729−36743

functions of EGCs and elevated levels of butyric acid in the colon of T2DM mice following inulin consumption in reducing colon inflammation.

The ENS comprises a multitude of EGCs, which play a pivotal role in colon inflammation. Upon activation, EGCs secrete pro-inflammatory cytokines, including TNF-α, IL-6, and LPS, thereby inducing pathological activation of EGCs. This activation triggers inflammation-related pathways, such as NF-κB, resulting in the release of pro-inflammatory cytokines. This inflammatory cascade amplifies inflammation, leading to systemic inflammation, including within the CNS.[43−45] In patients with T2DM, abnormal blood glucose levels, insulin resistance, intestinal dysbiosis, alterations in SCFA content, and resulting chronic inflammation collectively exert a substantial impact on the intestinal mucosal barrier and the intestinal−brain axis. It is evident that EGCs play a crucial role in modulating and controlling local inflammation, as well as maintaining the homeostasis of the intestinal and ENS environment.[6,46] The NF-κB pathway is likely the central regulator of these functions.

Based on existing research and scientific literature on the role of SCFAs, it has been reported that butyric acid has inhibitory effects on intestinal inflammation.[47] Building upon this knowledge, we hypothesized that butyric acid regulates the function of EGCs by inhibiting the nuclear translocation of NF-κB, thereby preventing its abnormal activation and exerting anti-inflammatory effects. Our hypothesis is supported by the observation that colonic levels of butyric acid were significantly higher in the DM-I group compared to the DM group and the difference of NF-κB pathway activation.

To summarize, our study demonstrates that colonic inflammation in mice with T2DM, induced by a high-fat diet combined with intraperitoneal injection of STZ, is closely associated with abnormal activation of EGCs and activation of the IKKβ/NF-κB pathway. The addition of inulin to the diet regulates the biological function of EGCs by restoring intestinal dysbiosis and normalizing the concentration of SCFAs in the colon. This improvement in colonic inflammation plays a positive role in T2DM mice with abnormal glucose metabolism, obesity, and systemic inflammation.

■ ASSOCIATED CONTENT

Supporting Information

The Supporting Information is available free of charge at https://pubs.acs.org/doi/10.1021/acsomega.3c03055.

Composition of different feeds; energy supply of protein, carbohydrates, and fat per kilogram of feeds; primer sequence; food consumption of each group; and PAS staining of colonic goblet cells in each group of mice at the 22nd week (PDF)

■ AUTHOR INFORMATION

Corresponding Authors

Han-Qiang Liu − *The Ministry of Education Key Lab of Hazard Assessment and Control in Special Operational Environment, The Shaanxi Provincial Key Laboratory of Environmental Health Hazard Assessment and Protection, The Shaanxi Provincial Key Laboratory of Free Radical Biology and Medicine, Department of Health Education and Management, School of Preventive Medicine, Air Force Medical University, Xi'an, Shaanxi 710032, China*; Email: liuhanqiangvip@163.com

Feng Wang − *The Ministry of Education Key Lab of Hazard Assessment and Control in Special Operational Environment, The Shaanxi Provincial Key Laboratory of Environmental Health Hazard Assessment and Protection, The Shaanxi Provincial Key Laboratory of Free Radical Biology and Medicine, Department of Health Education and Management, School of Preventive Medicine, Air Force Medical University, Xi'an, Shaanxi 710032, China*; Email: wfeng@fmmu.edu.cn

Authors

Meng-Ying Li − *The Ministry of Education Key Lab of Hazard Assessment and Control in Special Operational Environment, The Shaanxi Provincial Key Laboratory of Environmental Health Hazard Assessment and Protection, The Shaanxi Provincial Key Laboratory of Free Radical Biology and Medicine, Department of Health Education and Management, School of Preventive Medicine, Air Force Medical University, Xi'an, Shaanxi 710032, China; Department of Endocrinology, Xijing Hospital, Air Force Medical University, Xi'an, Shaanxi 710032, China*; orcid.org/0000-0003-0782-0987

Jia-Qi Duan − *The Ministry of Education Key Lab of Hazard Assessment and Control in Special Operational Environment, The Shaanxi Provincial Key Laboratory of Environmental Health Hazard Assessment and Protection, The Shaanxi Provincial Key Laboratory of Free Radical Biology and Medicine, Department of Health Education and Management, School of Preventive Medicine, Air Force Medical University, Xi'an, Shaanxi 710032, China*

Xiao-Hui Wang − *The Ministry of Education Key Lab of Hazard Assessment and Control in Special Operational Environment, The Shaanxi Provincial Key Laboratory of Environmental Health Hazard Assessment and Protection, The Shaanxi Provincial Key Laboratory of Free Radical Biology and Medicine, Department of Health Education and Management, School of Preventive Medicine, Air Force Medical University, Xi'an, Shaanxi 710032, China*

Meng Liu − *School of Environmental and Municipal Engineering, Xi'an University of Architecture and Technology, Xi'an 710055, China*

Qiao-Yi Yang − *The Ministry of Education Key Lab of Hazard Assessment and Control in Special Operational Environment, The Shaanxi Provincial Key Laboratory of Environmental Health Hazard Assessment and Protection, The Shaanxi Provincial Key Laboratory of Free Radical Biology and Medicine, Department of Health Education and Management, School of Preventive Medicine, Air Force Medical University, Xi'an, Shaanxi 710032, China*

Yan Li − *Department of Anatomy, Histology and Embryology and K. K. Leung Brain Research Centre, Air Force Medical University, Xi'an, Shaanxi 710032, China*

Kun Cheng − *Department of Endocrinology, Xijing Hospital, Air Force Medical University, Xi'an, Shaanxi 710032, China*

Complete contact information is available at: https://pubs.acs.org/10.1021/acsomega.3c03055

Author Contributions

M.Y.L. completed the initial draft along with Western Blot and cell experiments, J.Q.D. and M.L. conducted PCR and data collection. Y.L. performed tissue immunofluorescence staining, Q.Y.Y. and K.C. conducted statistical analysis. X.H.W., H.Q.L., and F.W. provided significant contributions to the research conception and design. The manuscript was revised by K.C., and all authors have read and approved the final version.

https://doi.org/10.1021/acsomega.3c03055
ACS Omega 2023, 8, 36729−36743

Funding

This work is partly supported by the project of the Shaanxi Provincial Science and Technology Department, China (grant no. 2021JM-231).

Notes

The authors declare no competing financial interest.

■ ACKNOWLEDGMENTS

This work was supported by the OE Biotech Co., Ltd (Shanghai, China) for providing the 16S rRNA sequencing and data.

■ ABBREVIATIONS

T2DM, type 2 diabetes mellitus; LPS, lipopolysaccharide; SCFAs, short-chain fatty acids; EGCs, enteric glial cells; ENS, enteric nervous system; CNS, central nervous system; STZ, streptozotocin; UPLC-ESI-MS/MS, ultra-performance liquid chromatography−electrospray ionization−tandem mass spectrometry; GC−MS, gas chromatography−mass spectrometry; H&E, hematoxylin−eosin; PAS, periodic acid-Schiff; IKKβ, κB inhibitor kinase β; IκBα, nuclear factor κB inhibitor α; NF-κB, nuclear factor κB; IL-1β, interleukin-1β; IL-6, interleukin-6; TNF-α, tumor necrosis factor; GFAP, glial fibrillary acidic protein; DAB, diaminobenzidine; GSP, glycated serum protein; RIPA, radio immunoprecipitation assay; BCA, bicinchoninic acid; FMT, fecal bacteria transplantation; PBS, phosphate-buffered saline; BSA, bovine serum albumin; PCoA, principal coordinates analysis; PCR, polymerase chain reactions; LEfSe, linear discriminant analysis effect size; KEGG, Kyoto Encyclopedia of Genes and Genomes; B/F, *Bacteroidetes*/*Firmicutes*; PPAR, proliferators-activated receptor; MAPK, mitogen-activated protein kinase

■ REFERENCES

(1) Magliano, D. J.; Boyko, E. J. IDF Diabetes Atlas 10th ed. scientific committee. *IDF Diabetes Atlas*, 10th ed.; IDF Diabetes Atlas; International Diabetes Federation: Brussels, 2021.

(2) Kundu, P.; Blacher, E.; Elinav, E.; Pettersson, S. Our Gut Microbiome: The Evolving Inner Self. *Cell* **2017**, *171* (7), 1481−1493.

(3) Shih, C.-T.; Yeh, Y.-T.; Lin, C.-C.; Yang, L.-Y.; Chiang, C.-P. Akkermansia Muciniphila Is Negatively Correlated with Hemoglobin A1c in Refractory Diabetes. *Microorganisms* **2020**, *8* (9), 1360.

(4) Chen, P.-C.; Chien, Y.-W.; Yang, S.-C. The Alteration of Gut Microbiota in Newly Diagnosed Type 2 Diabetic Patients. *Nutrition* **2019**, *63*−*64*, 51−56.

(5) Seguella, L.; Gulbransen, B. D. Enteric Glial Biology, Intercellular Signalling and Roles in Gastrointestinal Disease. *Nat. Rev. Gastroenterol. Hepatol.* **2021**, *18* (8), 571−587.

(6) Gonkowski, S.; Gajęcka, M.; Makowska, K. Mycotoxins and the Enteric Nervous System. *Toxins* **2020**, *12* (7), 461.

(7) Costa, D. V. S.; Moura-Neto, V.; Bolick, D. T.; Guerrant, R. L.; Fawad, J. A.; Shin, J. H.; Medeiros, P. H. Q. S.; Ledwaba, S. E.; Kolling, G. L.; Martins, C. S.; Venkataraman, V.; Warren, C. A.; Brito, G. A. C. S100B Inhibition Attenuates Intestinal Damage and Diarrhea Severity During Clostridioides Difficile Infection by Modulating Inflammatory Response. *Front. Cell. Infect. Microbiol.* **2021**, *11*, 739874.

(8) Chung, W. S. F.; Walker, A. W.; Louis, P.; Parkhill, J.; Vermeiren, J.; Bosscher, D.; Duncan, S. H.; Flint, H. J. Modulation of the Human Gut Microbiota by Dietary Fibres Occurs at the Species Level. *BMC Biol.* **2016**, *14*, 3.

(9) Yuan, Y.; Lu, L.; Bo, N.; Chaoyue, Y.; Haiyang, Y. Allicin Ameliorates Intestinal Barrier Damage via Microbiota-Regulated Short-Chain Fatty Acids-TLR4/MyD88/NF-KB Cascade Response in Acrylamide-Induced Rats. *J. Agric. Food Chem.* **2021**, *69* (43), 12837−12852.

(10) De Vadder, F.; Kovatcheva-Datchary, P.; Zitoun, C.; Duchampt, A.; Bäckhed, F.; Mithieux, G. Microbiota-Produced Succinate Improves Glucose Homeostasis via Intestinal Gluconeogenesis. *Cell Metab.* **2016**, *24* (1), 151−157.

(11) Liu, X.; Li, X.; Xia, B.; Jin, X.; Zou, Q.; Zeng, Z.; Zhao, W.; Yan, S.; Li, L.; Yuan, S.; Zhao, S.; Dai, X.; Yin, F.; Cadenas, E.; Liu, R. H.; Zhao, B.; Hou, M.; Liu, Z.; Liu, X. High-Fiber Diet Mitigates Maternal Obesity-Induced Cognitive and Social Dysfunction in the Offspring via Gut-Brain Axis. *Cell Metab.* **2021**, *33* (5), 923−938.e6.

(12) Lo Conte, M.; Antonini Cencicchio, M.; Ulaszewska, M.; Nobili, A.; Cosorich, I.; Ferrarese, R.; Massimino, L.; Andolfo, A.; Ungaro, F.; Mancini, N.; Falcone, M. A Diet Enriched in Omega-3 PUFA and Inulin Prevents Type 1 Diabetes by Restoring Gut Barrier Integrity and Immune Homeostasis in NOD Mice. *Front. Immunol.* **2023**, *13*, 1089987.

(13) Tang, Z.; Shao, T.; Gao, L.; Yuan, P.; Ren, Z.; Tian, L.; Liu, W.; Liu, C.; Xu, X.; Zhou, X.; Han, J.; Wang, G. Structural Elucidation and Hypoglycemic Effect of an Inulin-Type Fructan Extracted from Stevia Rebaudiana Roots. *Food Funct.* **2023**, *14* (5), 2518−2529.

(14) Chambers, E. S.; Byrne, C. S.; Morrison, D. J.; Murphy, K. G.; Preston, T.; Tedford, C.; Garcia-Perez, I.; Fountana, S.; Serrano-Contreras, J. I.; Holmes, E.; Reynolds, C. J.; Roberts, J. F.; Boyton, R. J.; Altmann, D. M.; McDonald, J. A. K.; Marchesi, J. R.; Akbar, A. N.; Riddell, N. E.; Wallis, G. A.; Frost, G. S. Dietary Supplementation with Inulin-Propionate Ester or Inulin Improves Insulin Sensitivity in Adults with Overweight and Obesity with Distinct Effects on the Gut Microbiota, Plasma Metabolome and Systemic Inflammatory Responses: A Randomised Cross-over Trial. *Gut* **2019**, *68* (8), 1430−1438.

(15) Sun, S.-C. The Non-Canonical NF-KB Pathway in Immunity and Inflammation. *Nat. Rev. Immunol.* **2017**, *17* (9), 545−558.

(16) Matoba, K.; Takeda, Y.; Nagai, Y.; Kawanami, D.; Utsunomiya, K.; Nishimura, R. Unraveling the Role of Inflammation in the Pathogenesis of Diabetic Kidney Disease. *Int. J. Mol. Sci.* **2019**, *20* (14), 3393.

(17) Charlton, A.; Garzarella, J.; Jandeleit-Dahm, K. A. M.; Jha, J. C. Oxidative Stress and Inflammation in Renal and Cardiovascular Complications of Diabetes. *Biology (Basel)* **2020**, *10* (1), 18.

(18) Yan, L.-J. NADH/NAD+ Redox Imbalance and Diabetic Kidney Disease. *Biomolecules* **2021**, *11* (5), 730.

(19) Alicic, R. Z.; Johnson, E. J.; Tuttle, K. R. Inflammatory Mechanisms as New Biomarkers and Therapeutic Targets for Diabetic Kidney Disease. *Adv. Chronic Kidney Dis.* **2018**, *25* (2), 181−191.

(20) Pichler, R.; Afkarian, M.; Dieter, B. P.; Tuttle, K. R. Immunity and Inflammation in Diabetic Kidney Disease: Translating Mechanisms to Biomarkers and Treatment Targets. *Am. J. Physiol. Renal Physiol.* **2017**, *312* (4), F716−F731.

(21) Neumiller, J. J.; Lienhard, F. J.; Alicic, R. Z.; Tuttle, K. R. Clinical Evidence and Proposed Mechanisms for Cardiovascular and Kidney Benefits from Sodium-Glucose Co-Transporter-2 Inhibitors. *touchREV Endocrinol.* **2022**, *18* (2), 106−115.

(22) Sazgarnejad, S.; Yazdanpanah, N.; Rezaei, N. Anti-Inflammatory Effects of GLP-1 in Patients with COVID-19. *Expert Rev. Anti-Infect. Ther.* **2022**, *20* (3), 373−381.

(23) Somm, E.; Montandon, S. A.; Loizides-Mangold, U.; Gaïa, N.; Lazarevic, V.; De Vito, C.; Perroud, E.; Bochaton-Piallat, M.-L.; Dibner, C.; Schrenzel, J.; Jornayvaz, F. R. The GLP-1R Agonist Liraglutide Limits Hepatic Lipotoxicity and Inflammatory Response in Mice Fed a Methionine-Choline Deficient Diet. *Transl. Res.* **2021**, *227*, 75−88.

(24) Wong, C. K.; Yusta, B.; Koehler, J. A.; Baggio, L. L.; McLean, B. A.; Matthews, D.; Seeley, R. J.; Drucker, D. J. Divergent Roles for the Gut Intraepithelial Lymphocyte GLP-1R in Control of Metabolism, Microbiota, and T Cell-Induced Inflammation. *Cell Metab.* **2022**, *34* (10), 1514−1531.e7.

(25) Alicic, R. Z.; Cox, E. J.; Neumiller, J. J.; Tuttle, K. R. Incretin Drugs in Diabetic Kidney Disease: Biological Mechanisms and Clinical Evidence. *Nat. Rev. Nephrol.* **2021**, *17* (4), 227−244.

(26) Fu, Y.; Ji, W.; Liu, Q.; Zhang, L.; Li, C.; Huan, Y.; Lei, L.; Gao, X.; Chen, L.; Feng, C.; Lei, L.; Zhai, J.; Li, P.; Cao, H.; Liu, S.; Shen, Z.

https://doi.org/10.1021/acsomega.3c03055
ACS Omega 2023, 8, 36729−36743

Voglibose Regulates the Secretion of GLP-1 Accompanied by Amelioration of Ileal Inflammatory Damage and Endoplasmic Reticulum Stress in Diabetic KKAy Mice. *Int. J. Mol. Sci.* **2022**, *23* (24), 15938.
(27) Wang, Y.; Fang, X.; Wang, S.; Wang, B.; Chu, F.; Tian, Z.; Zhang, L.; Zhou, F. The Role of O-GlcNAcylation in Innate Immunity and Inflammation. *J. Mol. Cell Biol.* **2023**, *14* (9), mjac065.
(28) Liu, J.; Ting, J. P.; Al-Azzam, S.; Ding, Y.; Afshar, S. Therapeutic Advances in Diabetes, Autoimmune, and Neurological Diseases. *Int. J. Mol. Sci.* **2021**, *22* (6), 2805.
(29) Qin, J.; Li, Y.; Cai, Z.; Li, S.; Zhu, J.; Zhang, F.; Liang, S.; Zhang, W.; Guan, Y.; Shen, D.; Peng, Y.; Zhang, D.; Jie, Z.; Wu, W.; Qin, Y.; Xue, W.; Li, J.; Han, L.; Lu, D.; Wu, P.; Dai, Y.; Sun, X.; Li, Z.; Tang, A.; Zhong, S.; Li, X.; Chen, W.; Xu, R.; Wang, M.; Feng, Q.; Gong, M.; Yu, J.; Zhang, Y.; Zhang, M.; Hansen, T.; Sanchez, G.; Raes, J.; Falony, G.; Okuda, S.; Almeida, M.; LeChatelier, E.; Renault, P.; Pons, N.; Batto, J.-M.; Zhang, Z.; Chen, H.; Yang, R.; Zheng, W.; Li, S.; Yang, H.; Wang, J.; Ehrlich, S. D.; Nielsen, R.; Pedersen, O.; Kristiansen, K.; Wang, J. A Metagenome-Wide Association Study of Gut Microbiota in Type 2 Diabetes. *Nature* **2012**, *490* (7418), 55−60.
(30) Natividad, J. M.; Lamas, B.; Pham, H. P.; Michel, M.-L.; Rainteau, D.; Bridonneau, C.; da Costa, G.; van Hylckama Vlieg, J.; Sovran, B.; Chamignon, C.; Planchais, J.; Richard, M. L.; Langella, P.; Veiga, P.; Sokol, H. Bilophila Wadsworthia Aggravates High Fat Diet Induced Metabolic Dysfunctions in Mice. *Nat. Commun.* **2018**, *9* (1), 2802.
(31) Tilg, H.; Zmora, N.; Adolph, T. E.; Elinav, E. The Intestinal Microbiota Fuelling Metabolic Inflammation. *Nat. Rev. Immunol.* **2020**, *20* (1), 40−54.
(32) Lan, Y.; Sun, Q.; Ma, Z.; Peng, J.; Zhang, M.; Wang, C.; Zhang, X.; Yan, X.; Chang, L.; Hou, X.; Qiao, R.; Mulati, A.; Zhou, Y.; Zhang, Q.; Liu, Z.; Liu, X. Seabuckthorn Polysaccharide Ameliorates High-Fat Diet-Induced Obesity by Gut Microbiota-SCFAs-Liver Axis. *Food Funct.* **2022**, *13* (5), 2925−2937.
(33) Liang, H.; Song, H.; Zhang, X.; Song, G.; Wang, Y.; Ding, X.; Duan, X.; Li, L.; Sun, T.; Kan, Q. Metformin Attenuated Sepsis-Related Liver Injury by Modulating Gut Microbiota. *Emerging Microbes Infect.* **2022**, *11* (1), 815−828.
(34) Ríos-Covián, D.; Ruas-Madiedo, P.; Margolles, A.; Gueimonde, M.; de Los Reyes-Gavilán, C. G.; Salazar, N. Intestinal Short Chain Fatty Acids and Their Link with Diet and Human Health. *Front. Microbiol.* **2016**, *7*, 185.
(35) Bäckhed, F.; Manchester, J. K.; Semenkovich, C. F.; Gordon, J. I. Mechanisms Underlying the Resistance to Diet-Induced Obesity in Germ-Free Mice. *Proc. Natl. Acad. Sci. U.S.A.* **2007**, *104* (3), 979−984.
(36) Zhao, T.; Gu, J.; Zhang, H.; Wang, Z.; Zhang, W.; Zhao, Y.; Zheng, Y.; Zhang, W.; Zhou, H.; Zhang, G.; Sun, Q.; Zhou, E.; Liu, Z.; Xu, Y. Sodium Butyrate-Modulated Mitochondrial Function in High-Insulin Induced HepG2 Cell Dysfunction. *Oxid. Med. Cell. Longevity* **2020**, *2020*, 1904609.
(37) Arkan, M. C.; Hevener, A. L.; Greten, F. R.; Maeda, S.; Li, Z.-W.; Long, J. M.; Wynshaw-Boris, A.; Poli, G.; Olefsky, J.; Karin, M. IKK-Beta Links Inflammation to Obesity-Induced Insulin Resistance. *Nat. Med.* **2005**, *11* (2), 191−198.
(38) Donath, M. Y.; Shoelson, S. E. Type 2 Diabetes as an Inflammatory Disease. *Nat. Rev. Immunol.* **2011**, *11* (2), 98−107.
(39) Sabio, G.; Das, M.; Mora, A.; Zhang, Z.; Jun, J. Y.; Ko, H. J.; Barrett, T.; Kim, J. K.; Davis, R. J. A Stress Signaling Pathway in Adipose Tissue Regulates Hepatic Insulin Resistance. *Science* **2008**, *322* (5907), 1539−1543.
(40) Akash, M. S. H.; Shen, Q.; Rehman, K.; Chen, S. Interleukin-1 Receptor Antagonist: A New Therapy for Type 2 Diabetes Mellitus. *J. Pharm. Sci.* **2012**, *101* (5), 1647−1658.
(41) Esser, N.; Paquot, N. [Inflammation, obesity and type 2 diabetes. Role of the NLRP3 inflammasome and gut microbiota]. *Rev. Med. Liege* **2022**, *77* (5−6), 310−315.
(42) Scheithauer, T. P. M.; Rampanelli, E.; Nieuwdorp, M.; Vallance, B. A.; Verchere, C. B.; van Raalte, D. H.; Herrema, H. Gut Microbiota as a Trigger for Metabolic Inflammation in Obesity and Type 2 Diabetes. *Front. Immunol.* **2020**, *11*, 571731.
(43) Neunlist, M.; Rolli-Derkinderen, M.; Latorre, R.; Van Landeghem, L.; Coron, E.; Derkinderen, P.; De Giorgio, R. Enteric Glial Cells: Recent Developments and Future Directions. *Gastroenterology* **2014**, *147* (6), 1230−1237.
(44) Coelho-Aguiar, J. d. M.; Bon-Frauches, A. C.; Gomes, A. L. T.; Veríssimo, C. P.; Aguiar, D. P.; Matias, D.; Thomasi, B. B. d. M.; Gomes, A. S.; Brito, G. A. d. C.; Moura-Neto, V. The Enteric Glia: Identity and Functions. *Glia* **2015**, *63* (6), 921−935.
(45) Sharkey, K. A. Emerging Roles for Enteric Glia in Gastrointestinal Disorders. *J. Clin. Invest.* **2015**, *125* (3), 918−925.
(46) Seguella, L.; Pesce, M.; Capuano, R.; Casano, F.; Pesce, M.; Corpetti, C.; Vincenzi, M.; Maftei, D.; Lattanzi, R.; Del Re, A.; Sarnelli, G.; Gulbransen, B. D.; Esposito, G. High-Fat Diet Impairs Duodenal Barrier Function and Elicits Glia-Dependent Changes along the Gut-Brain Axis That Are Required for Anxiogenic and Depressive-like Behaviors. *J. Neuroinflammation* **2021**, *18* (1), 115.
(47) Wang, X.; Duan, C.; Li, Y.; Lu, H.; Guo, K.; Ge, X.; Chen, T.; Shang, Y.; Liu, H.; Zhang, D. Sodium Butyrate Reduces Overnutrition-Induced Microglial Activation and Hypothalamic Inflammation. *Int. Immunopharmacol.* **2022**, *111*, 109083.

https://doi.org/10.1021/acsomega.3c03055
ACS Omega 2023, 8, 36729−36743